CHINESE OPTICS LETTERS

Vol. 20, No. 5 | May 2022

High signal-to-noise ratio fiber laser at 1596 nm based on a Bi/Er/La co-doped silica fiber

Lei Yang (杨 磊), Jianxiang Wen (文建湘)*, Yan Wu (吴 妍), Ying Wan (万 英), Longzhao Zeng (曾龙钊), Wei Chen (陈 伟), Fufei Pang (庞拂飞), Xiaobei Zhang (张小贝), and Tingyun Wang (王廷云)

Laboratory of Specialty Fiber Optics and Optical Access Networks, School of Communication and Information Engineering, Shanghai University, Shanghai 200444, China

*Corresponding author: wenjx@shu.edu.cn

Received January 6, 2022 | Accepted March 7, 2022 | Posted Online March 26, 2022

We fabricate a high-performance Bi/Er/La co-doped silica fiber with a fluorescence intensity of −33.8 dBm and a gain coefficient of 1.9 dB/m. With the utilization of the fiber as a gain medium, a linear-cavity fiber laser has been constructed, which exhibits a signal-to-noise ratio of 74.9 dB at 1596 nm. It has been demonstrated that the fiber laser has a maximum output power of 107.4 mW, a slope efficiency of up to 17.0%, and a linewidth of less than 0.02 nm. Moreover, an all-fiber single-stage optical amplifier is built up for laser amplification, by which the amplified laser power is up to 410.0 mW with pump efficiency of 33.8%. The results indicate that the laser is capable of high signal-to-noise ratio and narrow linewidth, with potential applications for optical fiber sensing, biomedicine, precision measurement, and the pump source of the mid-infrared fiber lasers.

Keywords: Bi/Er/La co-doped silica fiber; high signal-to-noise ratio laser; narrow linewidth.
DOI: 10.3788/COL202220.051402

1. Introduction

With the development of dense wavelength division multiplexing technology, the transmission capacity of the communication system has been increasingly expanded. Compared with the traditional C-band erbium-doped fiber (EDF) amplifier[1,2], the L-band EDF amplifier can significantly broaden the original gain bandwidth and improve the channel capacity[3,4]. In recent time, the L-band multiplexing technology and devices have tremendously aroused researchers' interest because of their potential applications in optical signal processing and optical fiber communication[5,6], including the study of the fiber laser[7]. Moreover, the fiber laser has many merits of low loss, flexible wavelength tuning, high optical signal-to-noise ratio (OSNR), and narrow bandwidth[8–11], which has driven several applications in optical fiber sensing[12], optical communication[13], biomedicine[14], and accurate measurement[15]. In 2001, Fujimoto *et al.* reported bandwidth luminescence properties of Bi-doped silica materials[16]. Bi-doped materials have realized ultra-wideband near infrared, covering the whole low-loss window in the wavelength range of 900–1800 nm[17] and become one of the most promising active media in this wide band. Er-doped materials are considered as the most widely used gain light-emitting media[18], and co-doping Bi is expected to improve the luminous efficiency and overcome the inherent limitation of the gain bandwidth of the EDF amplifier. Also, Er-doped or Bi/Er co-doped fiber can be used for in-fiber laser systems to achieve L-band lasers[19–21]. However, these lasers basically have poor anti-noise performance and low output power. Thus, in order to adapt to high-speed and large-capacity optical communication systems, a novel co-doped fiber operating at the L-band needs to be developed to realize L-band lasers with the admirable characteristics of low noise and narrow linewidth.

In this paper, we fabricate a Bi/Er/La co-doped silica fiber (BELDF), use it as a gain medium to establish a linear-cavity laser system, and study its laser performances. Furthermore, we build an optical amplifier system based on the laser as a signal light source and explore the amplification performances.

2. Fabrication and Properties of the Fibers

The BELDF is fabricated by modified chemical vapor deposition (MCVD) method combined with atomic layer deposition (ALD) technology[22]. Firstly, based on the ALD doping technology, the precursors of Bi, Er, La, and Al ions are introduced into a substrate tube and chemically react with deionized water to produce the corresponding oxides of these ions. Secondly, these oxides are deposited alternately and multi-layered to control the concentration of doped ions. Thirdly, it is shrunk into a solid doped preform by the MCVD method at high temperature. Finally, the preform is drawn to the BELDF.

In order to evaluate the content of elements in the home-made BELDF, the elemental composition is tested across the cross section of fiber by an electron probe micro-analyzer (EPMA-8050G, Shimadzu, Japan). The doping concentrations (atomic fractions) of Bi, Er, La, and Al atoms are 0.007%, 0.016%, 0.002%, and 0.412%, respectively. For the EDF, doping Al ions can make the fluorescence spectrum smoother and increase the bandwidth[23,24], doping La ions can avoid the cluster effect of Er ions, thus inhibiting the concentration quenching and improving the pumping efficiency[25], and doping Bi ions can increase the pump absorption efficiency of Er ions[26]. Figure 1(a) shows the refractive index distribution and cross-section image of the BELDF. The core and cladding diameters are 8.7 μm and 125.0 μm, respectively. The refractive index difference between the core and cladding layer is approximately 0.0040. Figure 1(b) shows the absorption spectrum of the BELDF, in which four typical absorption peaks of the Er ion exist at 653 nm, 796 nm, 978 nm, and 1529 nm, respectively. Those absorptions correspond to $^4I_{15/2} \rightarrow {}^4F_{9/2}$, $^4I_{9/2}$, $^4I_{11/2}$, and $^4I_{13/2}$. Especially, the absorption coefficient can reach 10.0 dB/m at 978 nm, which can ensure that the pump power is utilized effectively. According to the absorption spectrum, the estimated background loss is approximately 0.007 dB/m. In addition, the absorption bands of 800 nm, 1000 nm, and 1530 nm are broadened compared to the commercial EDF, indicating that there may be energy transfer between Bi ions and Er ions, which can improve the absorption efficiency of the BELDF, and Bi ions, and their surrounding Al ions, Si ions, and Ge ions can form luminescent centers to expand the bandwidth[27–30]. La ions can improve the dispersion of Er ions, reduce the 'cluster effect' of Er ions, and increase the luminous efficiency of Er ions. The interaction of La ions and Al ions can increase the energy level splitting of Er ions and expand the fluorescent bandwidth. Furthermore, the excitation–emission spectra and fluorescence

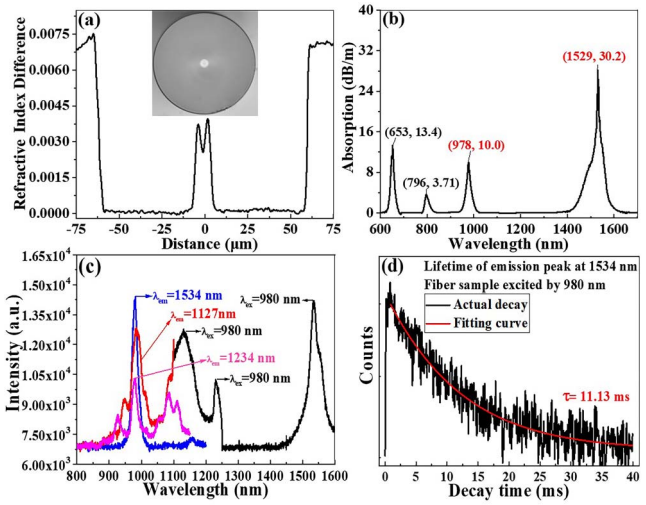

Fig. 1. (a) Refractive index distribution and the cross-sectional image (inset), (b) absorption spectrum, (c) excitation–emission spectra, and (d) fluorescence decay curves of the BELDF.

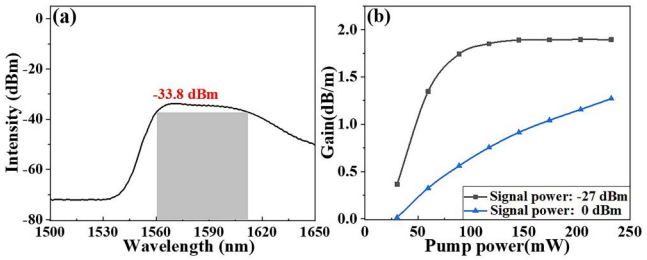

Fig. 2. (a) Fluorescence spectrum pumped by 980 nm laser and (b) the gain coefficient at different signal light powers as a function of pump power of the BELDF.

decay curve of the BELDF are measured using a fluorescence spectrophotometer (Edinburgh FLS-980, England), as shown in Figs. 1(c) and 1(d), respectively. As shown in Fig. 1(c), the three emission spectra excited at 1127 nm, 1234 nm, and 1534 nm present excitation peaks at 980 nm. In contrast, the emission peaks excited at 980 nm present broadband peaks at 1127 nm and 1234 nm. Especially, the excitation and emission peaks located at 980 nm and 1534 nm could originate from the electronic transitions between the $^4I_{13/2}$ and $^4I_{15/2}$ energy levels of Er ions, and the emission peaks located at 1127 nm and 1234 nm can be attributed to the electronic transitions between $^3P_1$ and $^3P_0$ of the Bi ion and the fluorescence lifetime of Er to the doping of Bi ions[31].

In order to explore the luminescence and gain characteristics, the fluorescence spectrum and gain coefficient of the BELDF are tested, as shown in Figs. 2(a) and 2(b). Note that the maximum intensity of the fluorescence spectrum is up to −33.8 dBm, and 3 dB bandwidth can reach 50 nm (1560–1610 nm) at the optimal fiber length of 15 m, indicating a great flatness of the spectrum, which can be applied for an L-band broad-spectrum light source[32]. Note that the gain coefficients of the BELDF are 1.9 dB/m at the signal light power of −27 dBm. When the signal power is 0 dBm and the pump power is 252 mW, there is no gain saturation. When the pump power continues to be increased, gain saturation will occur, implying a good gain characteristic, which is a footstone of the fiber laser and amplifier.

3. Laser and Amplification Performances

The linear-cavity fiber laser system is built up, as shown in the top box of Fig. 3. A 980 nm pump1 with the maximum output power of 685 mW supplies the sufficient pump power for the system. A wavelength division multiplexer (WDM) is used to combine the pump light and reflected light into BELDF1 that is used as a gain medium. The combination of a fiber Bragg grating (FBG), whose central wavelength is 1596 nm and reflectivity is 60%, and a 3 dB coupler forms a lasing cavity. An isolator (ISO) ensures the one-directional transmission of the signal light and the stability of the laser output. The output spectra and power of the laser are measured by an optical spectrum analyzer (OSA, AQ6370, Yokoga, Japan) with a resolution of 0.02 nm and a power meter (PM, PM100D, Thorlabs, USA), respectively.

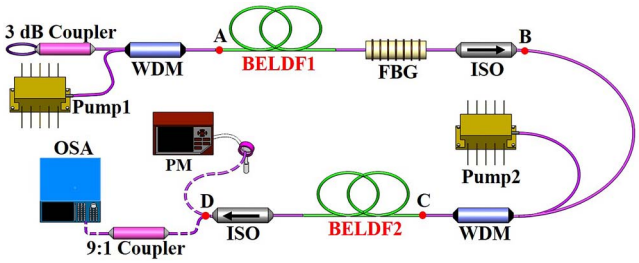

Fig. 3. Schematic of the 1596 nm fiber laser and optical amplification.

Firstly, the length of BELDF1 is changed in the range of 5–12 m, and the pump power into the BELDF1 at position 'A' and the corresponding 1596 nm laser output power at position 'B' are recorded, as shown in Fig. 4(a). Note that the laser output powers increase linearly with the increase of the input pump power, of which the slope efficiencies are 14.6%, 17.0%, 15.8%, 14.5%, and 13.8% with the BELDF1 length of 5, 6, 7, 9, and 12 m, respectively. The slope efficiency and the maximum output power as functions of the BELDF1 length are also measured, as shown in Fig. 4(b). As the BELDF1 length increases, the slope efficiency and maximum output power both exhibit a trend of increase first and then decrease, during which the optimal length is around 6 m. The main reason is that when the BELDF1 is relatively short, the fiber gain is limited, resulting in correspondingly larger threshold power and lower slope efficiency of the fiber laser. When BELDF1 is relatively long, the fiber absorption is high, resulting in the loss of optical power. Therefore, the 6-m-long BELDF1 can achieve the gain–loss matching, under which the slope efficiency and the maximum output power can reach 17.0% and 107.4 mW, respectively.

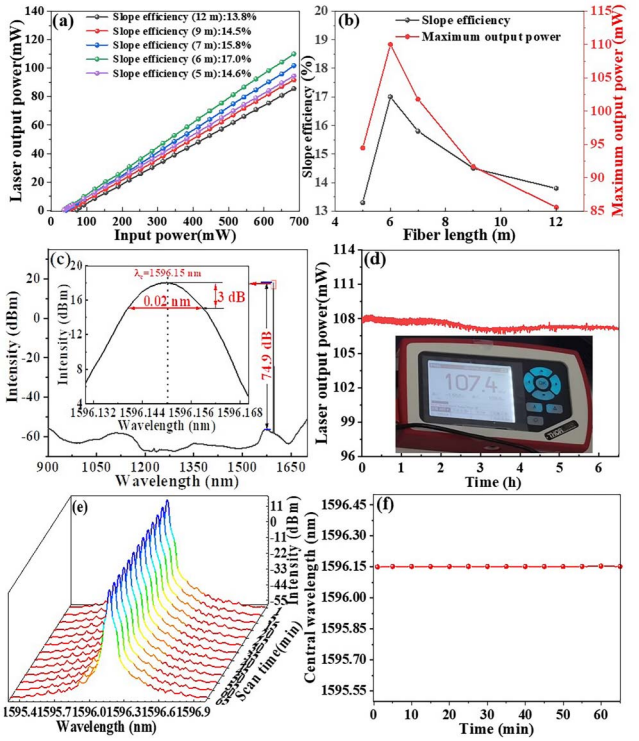

Fig. 4. Laser characteristics. (a) Laser output powers as a function of input pump powers with different lengths of BELDF1, (b) slope efficiency and maximum output power as functions of the BELDF1 length, (c) output spectra of the laser with a 6-m-long BELDF1 under maximum output power, (d) laser stability monitored within 6.5 h, (e) laser stability monitored within 65 min, and (f) fluctuation of the lasing center wavelength.

Under the optimal length of BELDF1, the laser output spectrum in the range of 900–1700 nm is recorded, as shown in Fig. 4(c). One can see no laser peak presence around 980 nm in the spectrum, implying that the pump light at 980 nm is completely converted in BELDF1. In addition, there is a narrow and strong laser peak observed with a central wavelength of 1596.15 nm and OSNR of 74.9 dB. The high OSNR performance mainly benefits from the simple laser configuration and excellent pump with a good side-mode-suppression ratio. Furthermore, the spectrum in the range of 1596.13–1596.17 nm is sampled to elucidate the laser characteristics, as shown in the inset of the Fig. 4(c). Note that the 3 dB linewidth of the laser peak is approximately 0.02 nm, which satisfies the narrow-linewidth condition of the fiber laser. Moreover, the output power of the high signal-to-noise ratio laser is continuously monitored for 6.5 h, as shown in Fig. 4(d). The fluctuation of the output power is less than 1.5%. At the same time, the wavelength stability of the 1596 nm fiber laser was continuously monitored every 5 min over 65 min using an OSA with a resolution of 0.02 nm, as shown in Fig. 4(e). The fluctuation of the lasing center wavelength was less than 0.01 nm, as shown in Fig. 4(f), which means that laser output is quite stable.

Table 1 summarizes the property parameters of the reported L-band fiber lasers. The laser structure and the active fibers' length are distinguishing, so the obtained lasers have different properties. Note that our laser has a slope efficiency of 17.0% and a laser output power of 107.4 mW, which are better than those parameters of linear-cavity lasers. Also note that the OSNR and 3 dB linewidth of our laser are over 74.9 dB and less than 0.02 nm, which are higher than those of any other lasers. Compared with the lasers reported in the Table 1, our 1596 nm fiber laser exhibits competitive performances in terms of slope efficiency, output power, OSNR, and 3 dB linewidth, mainly due to our home-made BELDF, which is doped with appropriate concentrations of Bi, Er, La, and Al ions. Bi ions can increase the pump absorption efficiency of Er ions; Al ions can make the fluorescence spectrum flatter and increase the bandwidth; La ions can suppress the concentration quenching phenomenon of high-concentration Er ions doping.

Subsequently, the 1596 nm laser with maximum output power is utilized as a signal light, and the optical amplification system is built up, as shown in the Fig. 3. A 980 nm pump2 with the maximum output power of 1020 mW provides the pump power for the amplification system. BELDF2 and BELDF1 are identical fibers. A 9:1 coupler that can reduce the output power to prevent it from exceeding the rated power of the OSA is connected to the end of the system. In the experiment, the length of BELDF2 is varied from 5 to 8 m, and the relationship between the amplified laser output power at position 'D' and the input

Table 1. Property Parameters of the Reported L-Band Fiber Lasers.

Central Wavelength (nm)	Fiber Length (m)	Slope Efficiency (%)	Output Power/Input Pump Power (mW)	Threshold Power (mW)	OSNR (dB)	3 dB Linewidth (nm)	Refs.
1595[a]	8.18	/	5.83/233	/	56	9.1	[33]
1610[a]	8	~6.2	308/5000	/	35	1.06	[34]
1567[a]	45	~33.7	91/270	/	/	0.03	[35]
1614[b]	2	~2.8	52.4/2500	/	~50	/	[36]
1582[b]	15	13.5	~11.2/100	15	~50	/	[37]
1595[b]	10	/	9.1/100	23.4	~40	/	[38]
1596[b]	6	17.0	107.4/685	~35	74.9	< 0.02	This work

[a]Ring-cavity laser system.

[b]Linear-cavity laser system.

pump power at position 'C' is recorded at different lengths of BELDF2, as shown in Fig. 5(a). Note that the amplified laser output powers increase linearly with the increase of the pump power. Also note that the pump efficiency is 31.5%, 33.8%, and 32.2% with the BELDF2 length of 5, 6, and 8 m, respectively, and the corresponding maximum output powers are 381.5, 410.0, and 389.7 mW. Therefore, the optimal length of BELDF2 is around 6 m for laser amplification.

Finally, the spectral characteristics after laser amplification with the 6-m-long BELDF2 are explored, as shown in Fig. 5(b). The OSNR of the narrow-linewidth laser after laser amplification is 65.0 dB, which has a 10 dB reduction compared with pre-amplification, mainly resulting from the increase of amplified spontaneous emission after optical amplification. The specific laser spectrum ranging from 1596.10 to 1596.14 nm is recorded, as shown in the inset of Fig. 5(b). The 3 dB linewidth of the laser peak is still approximately 0.02 nm, and the central wavelength is located at about 1596.12 nm, which is not significantly different from the laser central wavelength before amplification. The results indicate that the laser performances are well-maintained after amplification.

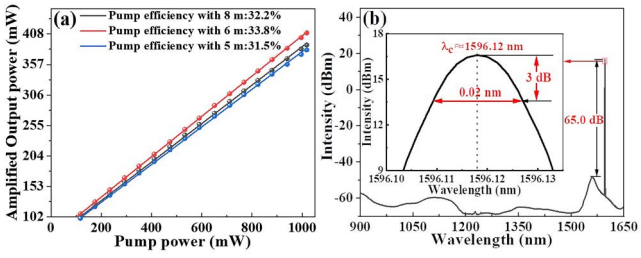

Fig. 5. (a) Amplified laser output power as a function of input pump power with different lengths of BELDF2 and (b) spectral characteristics of the amplified laser with BELDF2 length of 6 m.

4. Conclusion

In conclusion, we fabricate a BELDF using the MCVD method combined with ALD technology. Then, based on the fiber as a gain medium, we develop a 1596 nm high signal-to-noise ratio and narrow-linewidth laser with a linear-cavity structure. With the fiber length of 6 m, the laser operating at 1596 nm exhibits an output power of up to 107.4 mW, a slope efficiency of 17.0%, threshold power of ~35 mW, 3 dB linewidth of less than 0.02 nm, and OSNR of over 74.9 dB. The central wavelength and output power of the laser have remained almost unchanged for 6.5 h. Furthermore, the 1596 nm fiber laser with 107.4 mW output power is amplified as a signal light in an all-fiber optical amplification system. It can be obtained that the pump efficiency of the amplifier can reach 33.8%, and the maximum output power is up to 410.0 mW. Compared with the laser performance before amplification, the 3 dB linewidth of the amplified laser almost remains unchanged, and the output power is still stable, although the OSNR reduces by ~10 dB. In the future, we will further optimize the gain fiber parameters to realize a higher-quality and higher-efficiency narrow-linewidth fiber laser with higher output power and apply it in optical fiber sensing, precision measurement, and pump sources of the mid-infrared fiber lasers.

Acknowledgement

This work was supported by the National Key Research and Development Program of China (No. 2020YFB1805800), National Natural Science Foundation of China (Nos. 61975113, 61935002, 61735009, and 61705126), Project (No. D20031), and Shanghai Professional Technical Public Service Platform of Advanced Optical Waveguide Intelligent Manufacturing and Testing (No. 19DZ2294000).

References

1. Y.-E. Im, S.-R. Han, C.-S. Park, and K. Oh, "Temperature-dependent gain variation reduction in C-band erbium-doped fiber amplifier using phosphorus-erbium-doped silica fiber," IEEE Photon. Technol. Lett. **18**, 2087 (2006).
2. Y. N. Zhang, Y. F. Zhang, Q. L. Zhao, C. Li, C. S. Yang, Z. M. Feng, H. Q. Deng, E. B. Zhou, X. G. Xu, Kenneth K. Y. Wong, Z. M. Yang, and S. H. Xu, "Ultra-narrow linewidth full C-band tunable single-frequency linear-polarization fiber laser," Opt. Express **24**, 26209 (2016).
3. C. M. Lei, H. L. Feng, Y. Messaddeq, and S. LaRochelle, "Investigation of C-band pumping for extended L-band EDFAs," J. Opt. Soc. **37**, 2345 (2020).
4. J. H. Ji, L. Zhan, L. L. Yi, C. C. Tang, Q. H. Ye, and Y. X. Xia, "Low noise-figure gain-clamped L-band double-pass erbium-doped fiber ring lasing amplifier with an interleaver," J. Lightwave Technol. **23**, 1375 (2005).
5. E. Achaerandio, S. Jarabo, S. Abad, and M. López-Amo, "New WDM amplified network for optical sensor multiplexing," IEEE Photon. Technol. Lett. **11**, 1644 (1999).
6. W. Wu, Y. Yu, S. Hu, B. Zou, and X. Zhang, "All-optical format conversion for polarization and wavelength division multiplexed system," IEEE Photon. Technol. Lett. **24**, 1606 (2012).
7. Y. Wan, J. X. Wen, Y. H. Dong, C. Jiang, M. Jia, F. Z. Tang, N. Chen, Z. W. Zhao, S. J. Huang, F. F. Pang, and T. Y. Wang, "Exceeding 50% slope efficiency DBR fiber laser based on a Yb-doped crystal-derived silica fiber with high gain per unit length," Opt. Express **28**, 23771 (2020).
8. M. H. Al-Mansoori and M. A. Mahdi, "Multiwavelength L-band Brillouin–erbium comb fiber laser utilizing nonlinear amplifying loop mirror," J. Lightwave Technol. **27**, 5038 (2009).
9. T. Feng, M. M. Wang, D. L. Ding, and X. Steve Yao, "High OSNR and simple configuration dual-wavelength fiber laser with wide tunability in S+C+L band," Chin. Opt. Lett. **15**, 110602 (2017).
10. R. A. Perez-Herrera, A. Ullan, D. Leandro, M. Fernandez-Vallejo, M. A. Quintela, A. Loayssa, J. M. Lopez-Higuera, and M. Lopez-Amo, "L-band multiwavelength single-longitudinal mode fiber laser for sensing applications," J. Lightwave Technol. **30**, 1173 (2012).
11. Q. Zhao, L. Pei, Z. L. Ruan, J. J. Zheng, J. S. Wang, M. Tang, J. Li, and T. G. Ning, "Tunable and wavelength interval precisely controlled erbium-doped fiber laser by employing the fused taper technology," Chin. Opt. Lett. **20**, 011402 (2022).
12. J. H. Chen, D. R. Li, and F. Xu, "Optical microfiber sensors sensing mechanisms, and recent advances," J. Lightwave Technol. **37**, 2577 (2019).
13. K. Kikuchi, "Fundamentals of coherent optical fiber communications," J. Lightwave Technol. **34**, 157 (2016).
14. C. Wei, H. Shi, H. Luo, J. Xie, B. Zhai, F. Yuan, and Y. Liu, "Research progress of pulsed mid-infrared fiber lasers using two-dimensional materials," Chin. J. Lasers **44**, 0703009 (2017).
15. S. Ma, F. Xie, L. Chen, Y. Z. Wang, L. L. Dong, and K. Q. Zhao, "Development of dual-wavelength fiber ring laser and its application to step-height measurement using self-mixing interferometry," Opt. Express **24**, 5693 (2016).
16. Y. Fujimoto and M. Nakatsuka, "Infrared luminescence from bismuth-doped silica glass," Jpn. J. Appl. Phys. **40**, L279 (2001).
17. S. Firstov, S. Alyshev, M. Melkumov, K. Riumkin, A. Shubin, and E. Dianov, "Bismuth-doped optical fibers and fiber lasers for a spectral region of 1600-1800 nm," Opt. Lett. **39**, 6927 (2014).
18. Y. Li, K. Li, and J. Jin, "Influence of erbium-doped fiber's radiation effects on output characteristics of fiber source," Chin. J. Lasers **44**, 1206003 (2017).
19. Q. Zhao, L. Pei, Z. L. Ruan, J. J. Zheng, J. S. Wang, M. Tang, J. Li, and T. G. Ning, "Tunable and wavelength interval precisely controlled erbium-doped fiber laser by employing the fused taper technology," Chin. Opt. Lett. **20**, 011402 (2022).
20. K. K. Qureshi, X. H. Feng, L. M. Zhao, H. Y. Tam, C. Lu, and P. K. A. Wai, "C-band single-longitudinal mode lanthanum co-doped bismuth-based erbium doped fiber ring laser," Opt. Express **17**, 16352 (2009).
21. X. Y. Huang, H. H. Cheng, W. Luo, W. D. Zhang, M. Jiang, C. S. Yang, T. Yu, Z. P. Cai, Z. W. Xu, X. W. Shu, Z. M. Yang, J. R. Qiu, and S. F. Zhou, "Er-activated hybridized glass fiber for laser and senor in the extended wavebands," Adv. Opt. Mater. **9**, 2101394 (2021).
22. J. F. Xing, J. X. Wen, J. Wang, F. F. Pang, Z. Y. Chen, Y. Q. Liu, and T. Y. Wang, "All-fiber linear polarization and orbital angular momentum modes amplifier based on few-mode erbium-doped fiber and long period fiber grating" Chin. Opt. Lett. **16**, 100604 (2018).
23. L. Htein, W. W. Fan, and W. T. Han. "Broad gain of the Er/Al-doped fiber amplifier by pumping with a white light-emitting diode ," J. Lumin. **146**, 87 (2014).
24. Y. Waku, H. Ohtsubo, T. Takahashi, and A. Inoue, "An amorphous ceramic $Al_{32.4}Er_{7.6}O_{60}$ fiber with large viscous flow deformation and a high-strength nanocrystallized ceramic fiber," J. Mater. Sci. **36**, 2435 (2001).
25. Z. W. Jiang, J.-Y. Li, X. J. Liu, and H.-Q. Li, "Studies on characteristics of Er-La co-doped fiber," J. Optoelectron. Laser. **15**, 1038 (2004).
26. M. Y. Peng, N. Zhang, L. Wondraczek, J. R. Qiu, Z. M. Yang, and Q. Y. Zhang, "Ultrabroad NIR luminescence and energy transfer in Bi and Er/Bi co-doped germanate glasses," Opt. Express **19**, 20799 (2011).
27. R. Yang, M. F. Mao, Y. Zhang, Y. Z. Zhuang, K. Zhang, and J. R. Qiu. "Broadband near-infrared emission from Bi-Er-Tm co-doped germanate glasses," J. Non. Cryst. Solids. **357**, 2396 (2011).
28. T. M. Hau, X. Yu, D. C. Zhou, Z. G. Song, Z. W. Yang, R. F. Wang, and J. B. Qiu, "Super broadband near-infrared emission and energy transfer in Bi-Er co-doped lanthanum aluminosilicate glasses," Opt. Materials **35**, 487 (2013).
29. Z. M. Sathi, J. Z. Zhang, Y. H. Luo, J. Canning, and G. D. Peng, "Spectral properties and role of aluminium-related bismuth active centre (BAC-Al) in bismuth and erbium co-doped fiber," Opt. Mater. Express **5**, 1195 (2015).
30. Y. H. Luo, J. X. Wen, J. Z. Zhang, J. Canning, and G.-D. Peng, "Bismuth and erbium co-doped optical fiber with ultrabroadband luminescence across O-, E-, S-, C-, and L-bands," Opt. Lett. **37**, 3447 (2012)
31. H. H. Zhan, J. X. Wen, L. J. Chen, and Z. Y. Chen, "Research on Bi/Er co-doped silica optical fibers and its spectral characteristics," Opt. Commun. **406**, 3 (2018).
32. L. Yang, J. X. Wen, L. Z. Zeng, Y. Wu, S. J. Huang, F. F. Pang, X. B. Zhang, and T. Y. Wang, "Light sources in L-band based on a Bi/Er/La co-doped silica optical fiber," in *19th International Conference on Optical Communications and Networks (ICOCN)* (IEEE, 2021), p. 1.
33. Q. Huang, Z. Huang, M. Al Araimi, A. Rozhin, and C. Mou, "2.4 GHz L-band passively harmonic mode locked Er-doped fiber laser based on carbon nanotubes film," IEEE Photon. Technol. Lett. **32**, 121 (2020).
34. Y. H. Meng, G. Semaan, M. Salhi, A. Niang, K. Guesmi, Z.-C. Luo, and F. Sanchez, "High power L-band mode-locked fiber laser based on topological insulator saturable absorber," Opt. Express **23**, 23053 (2015).
35. G. R. Lin, J. Y. Chang, Y. S. Liao, and H. H. Lu, "L-band erbium-doped fiber laser with coupling-ratio controlled wavelength tunability," Opt. Express **14**, 9743 (2006).
36. S. J. Fu, X. S. Zhu, J. F. Wang, J. W. Wu, and M. H. Tong, "L-band wavelength-tunable Er^{3+}-doped tellurite fiber lasers," J. Lightwave Technol. **38**, 1435 (2020).
37. S.-K. Liaw, C.-S. Shin, and W.-F. Wu, "Tunable fiber laser using fiber Bragg gratings integrated carbon fiber composite with large tuning range," Opt. Laser Technol. **64**, 302 (2014).
38. M. H. Al-Mansoori, A. W. Naji, S. J. Iqbal, M. K. Abdullah, and M. A. Mahdi, "L-band Brillouin-erbium fiber laser pumped with 1480 nm pumping scheme in a linear cavity," Laser Phys. Lett. **4**, 371 (2006).